Structural Engineering and Mechanics, *Vol. 74, No. 2 (2020) 189-199*
DOI: https://doi.org/10.12989/sem.2020.74.2.189

Bridge-type structures analysis using RMP concept considering shear and bending flexibility

Mahmoud-Reza Hosseini-Tabatabaei*[1], Mohmmad Rezaiee-Pajand[2a] and Mahmoud R. Mollaeinia[1b]

[1]*Department of Civil Engineering, University of Zabol, Zabol, Iran,*
[2]*Department of Civil Engineering, Ferdowsi University of Mashhad, Mashhad, Iran*

(Received December 6, 2018, Revised October 15, 2019, Accepted November 17, 2019)

Abstract. Researchers have elaborated several accurate methods to calculate member-end rotations or moments, directly, for bridge-type structures. Recently, the concept of rotation and moment propagation (RMP) has been presented considering bending flexibility, only. Through which, in spite of moment distribution method, all joints are free resulting in rotation and moment emit throughout the structure similar to wave motion. This paper proposes a new set of closed-form equations to calculate member-end rotation or moment, directly, comprising both shear and bending flexibility. Furthermore, the authors program the algorithm of Timoshenko beam theory cooperated with the finite element. Several numerical examples, conducted on the procedures, show that the method is superior in not only the dominant algorithm but also the preciseness of results.

Keywords: bridge-frame; closed-form solution; continuous beam; finite element; Timoshenko beam

1. Introduction

Engineers have widely applied the bridge-type structures, continuous beams and bridge frames, with no sway in the construction industry. There exist two approximate and exact methods for analyzing these structures. The moment distribution method (Cross 1932), having a special place in structural engineering, represents a manual solution to estimate member-end moments. In this technique, to achieve the equilibrium conditions of a joint, it is released while all other joints restrained from rotation. Then, a part of the distributed moments is transmitted from the free joint (balanced joint) to neighbor clamped ones, resulting in unbalanced moments at the clamped joints. Iteratively, the restraining and releasing process of nodes reduces the deranged moments to meet the desired accurateness. Taking a more accuracy involves more iteration of the process, which significantly increases the analysis time. Thus, researchers have paid attention to developing simple exact methods for analysis of the bridges. Zuraski (1991) used the compatibility of joint deformations and the conjugate beam relationships to calculate member-end moments of symmetrical continuous beams with just constant flexural stiffness (EI). Dowell (2009) developed closed-form equations giving exact member-end moments for bridge structures with small depth-to-span ratio members. However, it cannot directly determine all member-end-moments at a joint where a column connected to, without taking into account static moment equilibrium equation. Rotation propagation's closed-form equations proposed by Hosseini-Tabatabaei and Rezaiee-Pajand (2012) facilitate precisely calculation of any member-end rotation of the bridges; yet, the slope-deflection method should be applied to obtain member-end moments. Mirfallah and Bozorgnasab (2015) proposed the slope distribution method, for the classical analysis of frames, in which only the nodal rotations (slopes) are distributed and no need to form and solve the system of algebraic equations. However, it is based on a Jacobi iterative procedure, thus the responses accuracy is depended on the number of iterations. In addition, it is not able to determine member-end moments, directly. Lately, Hosseini-Tabatabaei et al. (2017) used the concept of rotation propagation to derive moment closed-form equations, directly. Almayah (2018) presented an elastic analysis of continuous beams to determine the bending moment and deflection at various locations without the need to analyze the whole beam. He substituted three single span beams for each span of the continuous beam and determined the load on each of them by equations developed for this purpose. These equations are simple to apply to various loading and number of spans. Still, the spans' lengths should be equal and the results are approximate.

When a member of a bridge structure is thick relative to its length, shear effects noteworthy disturb deformations and moments. Gere (1963) took into account the shear effects. Moreover, Dowell and Johnson (2011) promoted Dowell's moment closed-form equations to deal with shear flexibility; nevertheless, for the joint having a column, the moment equilibrium equation have to be used.

In this research, a new set of formulation is derived for rotation and moment propagation to consider shear effects in addition to bending flexibility. Then, the formulation is set up into closed-form equations for calculation of

*Corresponding author, Ph.D.
E-mail: mr.htabatabaei@uoz.ac.ir,
mhoseini.tabatabaei@yahoo.com
[a] Ph.D. Professor
[b] Ph.D. Assistant Professor

ISSN: 1225-4568 (Print), 1598-6217 (Online)

member-end rotation or moment; individually, call rotation/moment propagation (RMP) method. Afterward, the authors have written a code for Timoshenko beam theory united with finite element (TMB-FE) method according to (Karttunen et al. 2016; Kaya and Dowling 2016; Romanoff et al. 2016). Finally, a comparison is performed between the exemplified results derived from the new scheme and TMB-FE analysis.

2. RMP Method

2.1 Rotation propagation concept

Consider a multi-span bridge frame, as shown in Fig. 1(a), subjected to an optional load transmitted by slabs and/or girders to it. The value of loads can be calculated by (such as) girder distribution factors (Tabsh and Mitchell 2016). Then, the loads are replaced by equivalent joint moments, Fig. 1(b). For arbitrary joint i, M_i derived from $M_i = M_i^E - M_i^F$, where M_i^E and M_i^F are the external joint moment and the sum of fixed-end moments at joint i, respectively. Now, assume all joints are free to rotate except fixed supports and the bridge is only subjected to M_i (see Fig. 1(c)), making a rotation $\theta_i^i = M_i / K_i$, where K_i is the rotational stiffness of joint i. The rotation propagates to the left and right side of i like a wave. Propagated rotation from i to its left neighbor, $i\text{-}1$, is computed by applying the rotation propagation factor, $C_\theta^{i(i-1)}$, as

$$\theta_i^{i-1} = C_\theta^{i(i-1)} . \theta_i^i \tag{1}$$

To how derive C_θ and K, see section 2.2.

2.2 RMP Formulation

In this section, we derive the governing equations and the basic parameters for exerting the shear effects in the RMP method.

2.2.1 Deriving of rotation propagation parameters

The bridge frame of Fig. 1(c) is cut open as Fig. 2. The rotational stiffness of the node i is equal to the sum of the rotational stiffness of elements connected to i including the left and right-hand sub-bridge frames, $K^{i(i-1)}$ and $K^{i(i+1)}$, respectively, and the column, K'^i,

$$K_i = K^{i(i-1)} + K^{i(i+1)} + K'^i \tag{2}$$

The span $i(i\text{-}1)$ of the left sub-bridge frame is taken out (Fig. 3), and a spring having rotational stiffness K_{i-1}^L is placed instead of the sub-bridge structure and the column connected to $i\text{-}1$, called beam-spring model, where K_{i-1}^L is

$$K_{(i-1)}^L = K^{(i-1)(i-2)} + K'^{(i-1)} \tag{3}$$

For the model, the relationship between rotations and moments including shear effects is written using the stiffness method as

$$\begin{bmatrix} k^{i(i-1)} & \alpha k^{i(i-1)} \\ \alpha k^{i(i-1)} & (K_{i-1}^L + k^{i(i-1)}) \end{bmatrix} \begin{Bmatrix} \theta_i^i \\ \theta_i^{i-1} \end{Bmatrix} = \begin{Bmatrix} M_i^{i(i-1)} \\ 0 \end{Bmatrix} \tag{4}$$

in which lowercase k and α are the rotational stiffness of member $i(i\text{-}1)$ and its carry-over factor, respectively, derived by (Gere 1963).

$$k^{i(i-1)} = \frac{4EI^{i(i-1)}}{L^{i(i-1)}} \left[\frac{2+\eta^{i(i-1)}}{2+4\eta^{i(i-1)}} \right] \tag{5}$$

$$\alpha^{i(i-1)} = \frac{1-\eta^{i(i-1)}}{2+\eta^{i(i-1)}} \tag{6}$$

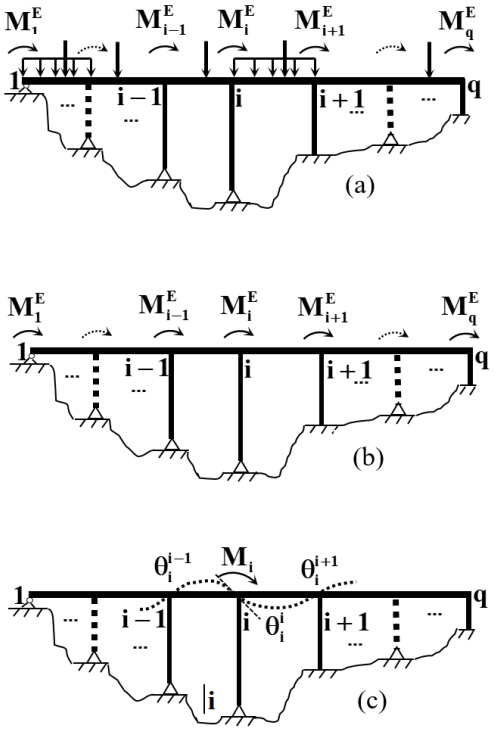

Fig. 1 A bridge frame (a) under an optional load and (b) subjected to contributed equivalent joint moments, and (c) the schematic illustration for the propagation of rotation (or moment).

where η exerting the shear effects is calculated by

$$\eta^{i(i-1)} = 12 c_s^{i(i-1)} \left(\frac{r_g^{i(i-1)}}{L^{i(i-1)}} \right)^2 (1+\upsilon) \tag{7}$$

Herein, c_s, v, r_g, and L are correspondingly the section shear constant, Poisson's ratio, the radius of gyration, and the span length in the member. Solving Eq. (4) in terms of the rotations leads to the following relationships.

$$\theta_i^i = \left(\frac{M_i^{i(i-1)}}{k^{i(i-1)}} \right) \left[\frac{\gamma_{(i-1)}^L + 1}{\gamma_{(i-1)}^L + 1 - (\alpha^{i(i-1)})^2} \right] \tag{8}$$

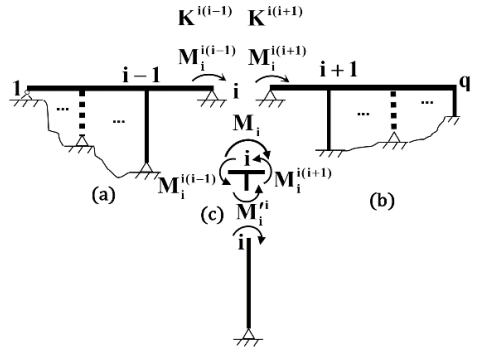

Fig. 2 Cut open the bridge frame at joint *i*.

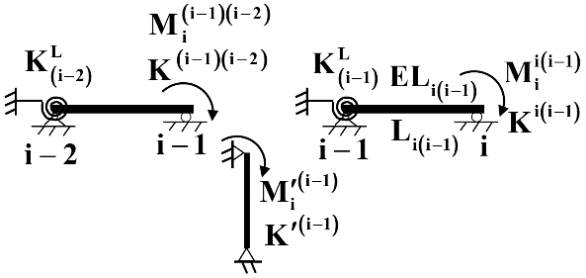

Fig. 3 Beam-spring simulation of the left sub-bridge structure of Fig. 2

$$\theta_i^{i-1} = \left(\frac{M_i^{i(i-1)}}{k^{i(i-1)}}\right)\left[\frac{-\alpha^{i(i-1)}}{\gamma_{(i-1)}^{L} + 1 - (\alpha^{i(i-1)})^2}\right] \tag{9}$$

where

$$\gamma_{(i-1)}^{L} = \frac{K_{(i-1)}^{L}}{k^{i(i-1)}} \tag{10}$$

and rotational stiffness of the beam-spring at i yields

$$K^{i(i-1)} = \frac{M_i^{i(i-1)}}{\theta_i^{i}} = k^{i(i-1)}\left[1 - \frac{(\alpha^{i(i-1)})^2}{\gamma_{(i-1)}^{L} + 1}\right] \tag{11}$$

The ratio of rotations at $i\text{-}1$ and i represents the rotation propagation factor as

$$C_{\theta}^{i(i-1)} = \frac{\theta_i^{i-1}}{\theta_i^{i}} = \frac{-\alpha^{i(i-1)}}{\gamma_{(i-1)}^{L} + 1} \tag{12}$$

Note, substituting α by 0.5 C_θ represents the rotation propagation factor for considering bending flexibility, only (Hosseini-Tabatabaei and Rezaiee-Pajand 2012).

2.2.2 Deriving moment propagation formulation

Recalling Figs. 1(c), 2 and 3, and distributing the equivalent moment M_i among the near end of the beam members and the column coupled to i as

$$M_i^{i(i-1)} = D^{i(i-1)} M_i,\ M_i^{i(i+1)} = D^{i(i+1)} M_i,\ M_i'^{i} = D'^{i} M_i \tag{13}$$

where $M_i^{i(i-1)}, M_i^{i(i+1)}$ and $M_i'^{i}$ represent the distributed moments and

$$D^{i(i-1)} = \left(\frac{K^{i(i-1)}}{K_i}\right),\quad D^{i(i+1)} = \left(\frac{K^{i(i+1)}}{K_i}\right),\quad D'^{i} = \left(\frac{K_i'}{K_i}\right) \tag{14}$$

$D^{i(i-1)}, D^{i(i+1)}$, and D'^{i} are correspondingly their moment free-distribution factors. Pay attention that definition of these factors is identical to what used by moment distribution method. However, they are naturally different, because in contrast to the moment distribution method all joints are free to rotate, except the fixed supports. Then, the distributed moment, $M_i^{i(i-1)}$, is propagated to the far end of the member $i(i\text{-}1)$ using the moment propagation factor, $C_M^{i(i-1)}$, as

$$M_i^{(i-1)i} = C_M^{i(i-1)} . M_i^{i(i-1)} \tag{15}$$

where

$$C_M^{i(i-1)} = \frac{\gamma_{(i-1)}^{L} \alpha^{i(i-1)}}{\gamma_{(i-1)}^{L} + 1 - (\alpha^{i(i-1)})^2} \tag{16}$$

Similarly, for the column at $i\text{-}1$, the propagated moment is obtained as

$$M'^{(i-1)} = -K'^{(i-1)} . \theta_i^{i-1} = C_{M'}^{i(i-1)} . M_i^{i(i-1)} \tag{17}$$

in which

$$C_{M'}^{i(i-1)} = \frac{-\gamma'^{L}_{(i-1)} \alpha^{i(i-1)}}{\gamma_{(i-1)}^{L} + 1 - (\alpha^{i(i-1)})^2} \tag{18}$$

where $C_{M'}^{i(i-1)}$ is the moment propagation factor of the column connected to $i\text{-}1$ and

$$\gamma'^{L}_{(i-1)} = \frac{K'^{(i-1)}}{k^{i(i-1)}} \tag{19}$$

Also, propagated moment to the near end of the next beam-spring model (see Fig. 3) is

$$M_i^{(i-1)(i-2)} = -K^{(i-1)(i-2)} . \theta_i^{i-1} = C_{M''}^{i(i-1)} . M_i^{i(i-1)} \tag{20}$$

where

$$C_{M''}^{i(i-1)} = -\frac{(\gamma_{(i-1)}^{L} - \gamma'^{L}_{(i-1)}) \alpha^{i(i-1)}}{\gamma_{(i-1)}^{L} + 1 - (\alpha^{i(i-1)})^2} \tag{21}$$

Note that the sum of the moment propagation factors is equal to zero which leads to the relationship of

$$C_M^{i(i-1)} = -(C_{M''}^{i(i-1)} + C_{M'}^{i(i-1)}) \tag{22}$$

If there is no column, $C_{M'}^{i(i-1)}$ is zero, and consequently $C_M^{i(i-1)} = -C_{M''}^{i(i-1)}$.

2.2.3 Closed-form equations of RMP method

Referring to Fig. 1(c) and Eq. (1), for an arbitrary joint, *m*, at the left side of i , we can write

$$\begin{aligned}\theta_i^{m} &= C_{\theta}^{(m+1)m} . \theta_i^{m+1} \\ &= C_{\theta}^{(m+1)m} . C_{\theta}^{(m+2)(m+1)} \ldots C_{\theta}^{i(i-1)} . \left[\frac{M_i}{K_i}\right] = \theta_i^{i} \prod_{j=m}^{i-1} C_{\theta}^{(j+1)j}\end{aligned} \tag{23}$$

Capital P_i, Π, indicates the multiplication of all rotation propagation factors from the lower to upper limits specified. Similarly, for propagated rotation of a subjective joint, m, at the right side of i, we have

$$\theta_i^m = C_\theta^{(m-1)m}.\theta_i^{(m-1)} = C_\theta^{(m-1)m}.C_\theta^{(m-2)(m-1)}...C_\theta^{i(i+1)}.[\frac{M_i}{K_i}] = \theta_i^i \prod_{j=i}^{m-1} C_\theta^{j(j+1)} \quad (24)$$

Here, for the general case of the bridge structure (Fig. 1(a)) carrying an optional load, the total rotation of the joint m is derived using the superposition principle as

$$\theta^m = [\sum_{i=1}^{m} \theta_i^i \prod_{j=i}^{m-1} C_\theta^{j(j+1)}] + [\sum_{i=m+1}^{q} \theta_i^i \prod_{j=m}^{i-1} (C_\theta^{(j+1)j}] \quad (25)$$

in which, q is the number of joints of the structure. Eq. (25) represents the first closed-form equation of RMP Method.

Remind Eqs. (15), (16), (18), and (21). The propagated moments of beam members at the left and right sides of an arbitrary joint m taken place at the left side of the joint i are

$$M_i^{mn} = \beta_L^{mn}.M_i^{i(i-1)} \prod_{j=i}^{m} C_{M''}^{j(j-1)} \quad (26)$$

where

$$\beta_L^{mn} = \begin{cases} C_M^{nm} & \text{if} \quad n = m+1 \\ C_{M''}^{(m+1)(n+1)} & \text{if} \quad n = m-1 \end{cases} \quad (27)$$

and for the column connected to m,

$$M_i'^m = C_{M'}^{(m+1)m}.M_i^{i(i-1)} \prod_{j=i}^{m} C_{M''}^{j(j-1)} \quad (28)$$

Now, consider Fig. 4 as a part of a bridge frame subjected to M_6 that shows a schematic procedure of the moment propagation from the node 6 to 3. The moment M_6^{65} resulted due to the distribution of M_6 among the near ends of members connected to joint 6, is propagated up to the node 3, using the moment propagation factors.

We can write a similar equation for propagation of the moment M_i to any joint m at the right side of the node i, as

$$M_i^{mn} = \beta_R^{mn}.M_i^{i(i+1)} \prod_{j=i}^{m} C_{M''}^{j(j+1)} \quad (29)$$

where

$$\beta_R^{mn} = \begin{cases} C_M^{nm} & \text{if} \quad n = m-1 \\ C_{M''}^{(m-1)(n-1)} & \text{if} \quad n = m+1 \end{cases} \quad (30)$$

and for the column connected to m, we have

$$M_i'^m = C_{M'}^{(m-1)m}.M_i^{i(i+1)} \prod_{j=i}^{m} C_{M''}^{j(j+1)} \quad (31)$$

The use of the superposition principle, when a freewill load acting on the bridge frame, leads to obtaining the total moments of the beams and the column connected to the node, as

$$M^{mn} = M_{mn}^F + M_m^{mn} + \beta_R^{mn}[\sum_{i=1}^{m-1} M_i^{i(i+1)} (\prod_{j=i}^{m-2} C_{M''}^{j(j+1)})] + \beta_L^{mn}[\sum_{i=m+1}^{q} M_i^{i(i-1)} (\prod_{j=m+1}^{i-1} C_{M''}^{(j+1)j})] \quad (32)$$

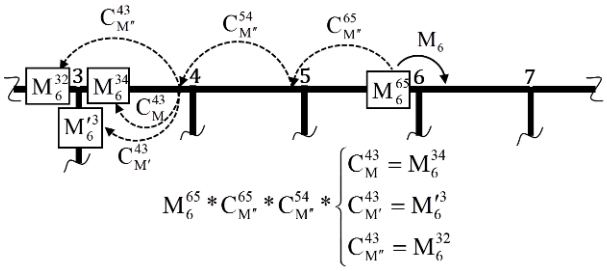

Fig. 4. A schematic diagram of moment propagation

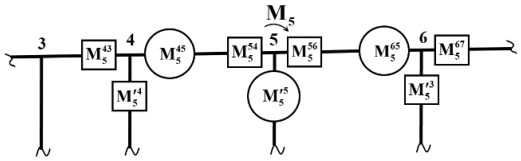

Fig. 5. Member-end moments, which can directly/indirectly be determined by Dowell's equations

$$M'^m = M_m'^F + M_m'^m + C_{M'}^{(m-1)m}.\sum_{i=1}^{m-1} M_i^{i(i+1)} \prod_{j=i}^{m-2} C_{M''}^{j(j+1)} + C_{M'}^{(m+1)m} \sum_{i=m+1}^{q} M_i^{i(i-1)} \prod_{j=m+1}^{i-1} C_{M''}^{(j+1)j} \quad (33)$$

where $M_m'^F$ is the fixed-end moment of the column jointed to m. These moments, for an arbitrary member ij under a point load on, are (Gere 1963).

$$M_{ij}^F = -\frac{Pbb'^2}{L^2}\left[\frac{1+(L/b')\eta}{1+2\eta}\right], \quad M_{ji}^F = \frac{Pb'b^2}{L^2}\left[\frac{1+(L/b)\eta}{1+2\eta}\right] \quad (34)$$

in which b is the distance from the left joint of the span to the point load, and $b' = L - b$.

In all closed-form equations, $\prod_i^n C_j = 1$ if $n < i$. The Eqs. (32) and (33) are the second and third closed-form equations of RMP method, respectively.

Seeking in RMP closed-form equations show that the used parameters have exact-certain values and there is not required to restrain and release the joints, repetitively, thus the RMP method is efficient. Moreover, the RMP method can directly obtain any member-end moment, at each joint, while Dowell's techniques (Dowell 2009; Dowell and Johnson 2011; Dowell and Johnson 2012) calculate some of them through closed-form equations, straightly and apply static moment equilibrium equations for others. For example, as shown in Fig. 5, Dowell's equations can

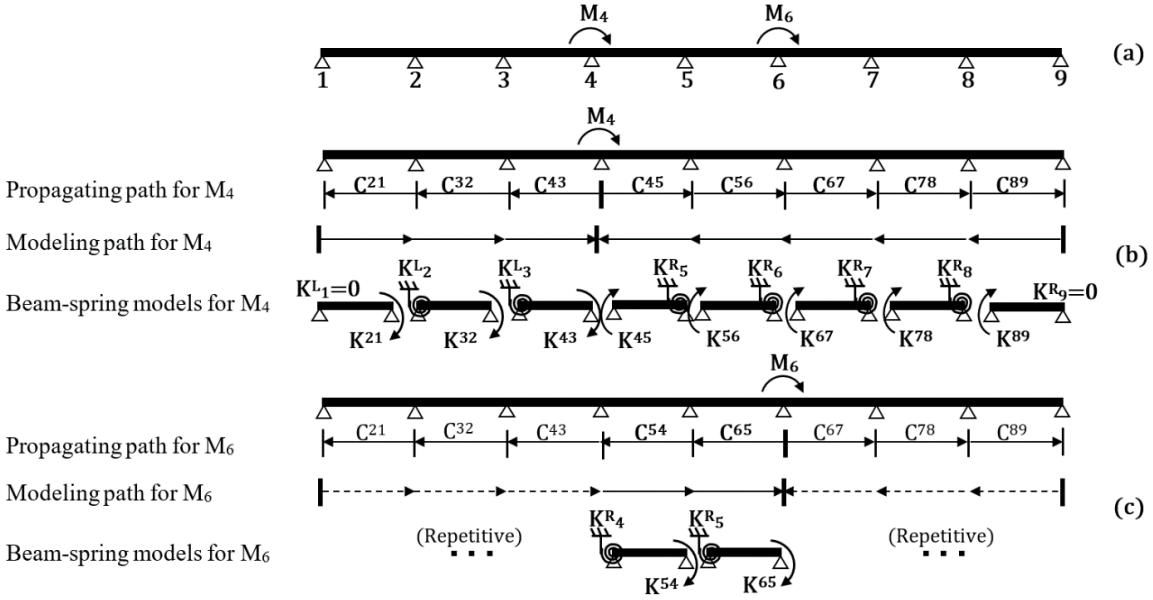

Fig. 6. The propagating and modeling paths

calculate the moments of, M_5^{56} and M_5^{54} for joint 5, directly but the moment of $M_5^{'5}$, denoted by circle, should be derived from moment equilibrium equation at 5.

2.3 Step-by-step process of RMP

Now, to perform hand solution and to more realize the concepts of RMP method, a step-by-step procedure is suggested as

1. Calculating fixed-end moment and rotational stiffness for all members, and equivalent joint moments for all joints.
2. Gaining the stiffness of equivalent springs, K^L and K^R, from left to right and vice versa, as well as, propagation factors, C_θ or C_M and free-distribution factors, D.
3. Selecting each joint i having equivalent node moment, M_i, and calculating rotation of joint i for rotation propagation analysis, or distributed moments for the moment propagation.
4. Computing the propagated rotations or moments from the joint i to other nodes.
5. Performing steps 3 and 4 for all loaded joints.
6. Summing the results of actions 3-5 to calculate member-end rotations or moments. Note that moment propagation procedure totalizes by adding fixed-end moments.

2.4 Paths of propagation and modelling

Consider a continuous beam carrying equivalent joint moments on nodes 4 and 6, shown in Fig. 6(a).

The rotation or moment propagates from the joints (e.g., node 4) towards ends while the beam-spring simulation and parameters calculation including the propagation factors and the rotational stiffness coefficients start from both ends of the structure.

The desirable parameters should only be derived one time in each direction. For example, to propagate the moment M_4 to point 1, it is necessary to compute K^{21}, K^{32}, K^{43}, C^{21}, C^{32}, and C^{43} (Fig. 6(b)). Then, for propagating the moment M_6 to the node 1; K^{54}, K^{65}, C^{54}, and C^{65} should be obtained only (Fig. 6(c)), and one can adopt K^{21}, K^{32}, K^{43}, C^{21}, C^{32}, and C^{43} from previous calculations.

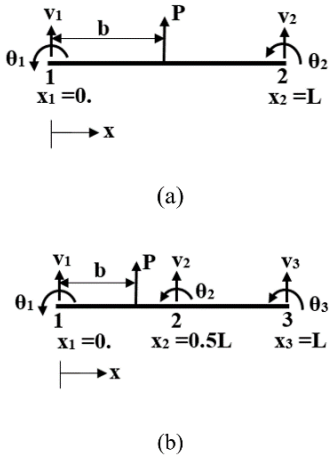

Fig. 7. (a) Two-node and (b) three-node Timoshenko beam finite elements

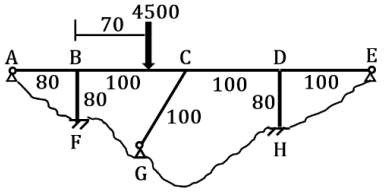

Fig. 8. The bridge frame used in examples 1 and 3

(a) Sub-structures DC, DH, and DE. (b) Sub-structures CB, CG, and CD.

Fig. 9. Modeling some parts of the bridge.

3. Timoshenko beam finite element formulation

Herein, we present the element-level formulation of TMB finite element in brief. Applying FE analysis, a bridge-type structure can be meshed by one dimensional (1D) element with n-node , a polynomial interpolates the desired quantity (such as deformation) over each, and adjacent segments share the degree of freedoms (DOFs) at connecting nodes (Eslami 2014).

Figs. 7(a)-(b) represent the configuration of a two-node element (2-NE) and a three-node element (3-NE) (Regueiro and Duan 2015), respectively, in which each node has two degrees of freedom, including one displacement and one rotation.

The stiffness matrix for both elements can be derived by (see Appendix)

$$[S]=\int_0^L [B]^T[M][B]dx \tag{35}$$

where

$$[M]=\begin{bmatrix} EI & 0 \\ 0 & \dfrac{GA}{c_S} \end{bmatrix} \tag{36}$$

EI and *GA* are respectively the flexural and shear rigidity of cross-sections, and *[B]* is the strain matrix. By rewriting Eq. (35) for a nodal demonstration we have

$$\begin{aligned} &[S]_{ij}=\int_0^L [B_i]^T[M][B_j]dx, \\ &i,j=1,2 \text{ for } 2-NE, \text{ and } 1,2,3 \text{ for } 3-NE \end{aligned} \tag{37}$$

in which the nodal strain matrix for a specified node, *m*, is

$$[B_m]=\begin{bmatrix} 0 & dN_m/dx \\ -dN_m/dx & N_m \end{bmatrix},\ m=i \text{ and/or } j \tag{38}$$

In above equation, N_m is the nodal shape function. The arrays of the shape functions accompanied by the nodal deformation vector and strain matrix are

$$[N]_{2-node}=[N_1 \quad N_2]=[1-\frac{x}{L},\frac{x}{L}] \tag{39}$$

$$\begin{aligned} &[N]_{3-node}=[N_1 \quad N_2 \quad N_3] \\ &=[(1-\frac{2x}{L})(1+\frac{x}{L}),(\frac{x}{L})(1-\frac{x}{L}),(\frac{-x}{L})(1-\frac{2x}{L})] \end{aligned} \tag{40}$$

Illustrating the vector of the nodal load, $\{f\}$, and the equivalent one, $\{f\}_{Eq}$, the elemental governing equation is

$$[S]\{d\}=\{f\}+\{f\}_{Eq} \tag{41}$$

where

$$\{d_m\}=\{v_m \quad , \quad \theta_m\}^T \tag{42}$$

$$\{f_m\}_{Eq}=\{N_m P \quad , \quad 0\}^T_{x=a} \tag{43}$$

where *P* is vertical point load on the elements (see Figs. 7(a)-(b)). In this paper, the authors provided a convenient computer program corresponding to each of the elements to analyse any bridge-type structure. Completing the process of finite element analysis consequences a set of algebraic equations to be solved, simultaneously. The number of which and the convergence of the analysis are dependent upon mesh refinement.

4. Examples

4.1 Example 1

Fig. 8 shows a bridge frame having deep members with $\eta_{AB}=\eta_{BF}=\eta_{DH}=0.298616$, $\eta_{BC}=\eta_{CD}=\eta_{DE}=\eta_{CG}=0.191114$, and $EI=1$ for all members.

The step-by-step procedure of rotation propagation is applied to determine member-end rotations as

Step 1) Fixed-end moments of the span BC are determined by Eq. (34), and then the equivalent joint moments are derived, M_B=33576.424 and M_C=-60923.576. Also, using Eqs. (5)-(6), k=0.0359781 and α=0.305133 are obtained for members AB, BF, and DH; and k=0.0317040 and α=0.369167 for the others.

Step 2) For the columns of BF and DH due to constraining joints of F and H, $\gamma=\infty$ resulted in equality of Eqs. (5) and (11), consequently $K'^B=K'^D=k^{BF}=k^{DH}$=0.0359781. For the column of CG pined at G, γ=0 thus, K'^C=0.0273833. For determination of rotation propagation parameters, the bridge is just modeled from A to C and E to B because the joints B and C have the equivalent moments, only. To demonstrate how to calculate the required parameters, for example, the calculation of parameters from E to C is presented as

a) Beam-spring model DE, Fig. 9(a)

$$K^R_E=0 \ \Rightarrow \ \gamma^R_E=0$$

$$K^{DE}=k^{DE}[1-(\alpha^{DE})^2/(\gamma^R_E+1)]=0.0273833$$

$$\Rightarrow C^{DE}_\theta=-\alpha^{DE}/(\gamma^R_E+1)=-0.3691665$$

$$C^{DH}_\theta=-\alpha^{DH}/(\infty+1)=0. \quad (Note: \ \gamma'_H=\infty)$$

b) Beam-spring model CD, Fig. 9(b)

$$K_D^R = K^{DE} + K'^D = 0.0633615,$$

$$\gamma_D^R = K_D^R / k^{DE} = 1.998526 \Rightarrow$$

$$K^{CD} = k^{CD}[1-(\alpha^{CD})^2/(\gamma_D^R+1)] = 0.0302631$$

$$C_\theta^{CD} = -\alpha^{CD}/(\gamma_D^R+1) = -0.123116$$

$$C_\theta^{CG} = -\alpha^{CG}/(\gamma_D^R+1) = -0.369167$$

Similarly, we compute the other parameters. Then, the rotational stiffness of joints is acquired. For instance

$$K_B = K^{BA} + K'^B + K^{BC} = 0.098777,$$

Step 3) The rotation at B produced by M_B is obtained, typed in column 3-row 6 of Table 1,

$$\theta_B^B = M_B / K_B = 339920.02$$

Step 4) The rotation θ_B^B propagates to the other joints (columns 2 and 4-6 of row 7 in Table 1) as

$$\theta_B^A = \theta_B^B.C_\theta^{BA} = -103720.9, \quad \theta_B^C = \theta_B^B.C_\theta^{BC} = -44526.35$$

$$\theta_B^D = \theta_B^C.C_\theta^{CD} = 5481.906, \quad \theta_B^E = \theta_B^D.C_\theta^{DE} = -2023.736$$

Step 5) Similarly, the steps 3-4 are repeated for the other loaded joint C.

Step 6) Total amount of rotation at any joint, produced by both (all) equivalent joint moments, are accessible in the tenth row of Table 1. For example

$$\theta_A = \theta_B^A + \theta_C^A = -128373.3$$

$$\theta_B = \theta_B^B + \theta_C^B = 420711.96$$

To directly determine a single member-end-rotation (such as θ_D), it is not necessary to calculate all rotation propagation parameters. Those values need to obtain θ_D were bolded in Table 1. It is just sufficient to institute them in

$$\theta_D = [M_B / K_B][C_\theta^{BC} C_\theta^{CD}] + [M_C / K_C][C_\theta^{CD}] = 90731.348$$

4.2 Example 2

The bridge of example 1 is analyzed by moment propagation method for directly determining member-end moments. Thus,

Step 1) The fixed-end moments, the equivalent joint moments, rotational stiffness of members and their carry-over factors are as equal as example 1.

Step 2) The values of γ, all rotational stiffness of the beam-spring models from left to right and vice versa and the rotational stiffness of joints are the same as example 1.The values of γ' and moment propagation and free-distribution factors should be determined. For example, we can write for

a) beam-spring model DE

$$C_M^{DE} = (-\gamma_E^R.\alpha^{DE})/[\gamma_E^R + 1 - (\alpha^{DE})^2] = 0.,$$

$$C_{M'}^{DE} = C_{M''}^{DE} = 0.$$

,

b) and for beam-spring model CD

$$\gamma_D^R = K_E^R / k^{DE} = 1.998526,$$

$$\gamma_D'^R = K'^D / k^{DE} = 1.13481$$

$$C_M^{CD} = \frac{-\gamma_D^R \alpha^{CD}}{\gamma_D^R + 1 - (\alpha^{CD})^2} = 0.257766,$$

$$C_{M''}^{CB} = \frac{-(\gamma_D^R - \gamma_D'^R)\alpha^{CD}}{\gamma_D^R + 1 - (\alpha^{CD})^2} = -0.111400$$

$$C_{M'}^{CB} = \frac{-\gamma_D'^R \alpha^{CD}}{\gamma_D^R + 1 - (\alpha^{CD})^2} = -0.146366$$

In the same way, one can obtain the other moment propagation parameters, written in table 2. Now, the values of the free-distribution factors are derived. For instance

$$D^{CB} = K^{CB} / K_C = 0.34481,$$

$$D^{CD} = K^{CD} / K_C = 0.343958,$$

$$D^{CG} = D'^C = K'^C / K_C = 0.311233,$$

$$D^{BA} = K^{BA} / K_B = 0.33032,$$

$$D^{BC} = K^{BC} / K_B = 0.30544,$$

$$D^{BF} = D'^C = K'^B / K_B = 0.36423$$

Step 3) Distributing M_B among all members connected to joint B,

$$DM_B^{BA} = M_B.D^{BA} = 11091.024,$$

$$DM_B^{BC} = M_B.D^{BC} = 10255.714$$

$$DM_B^{BF} = M_B.D'^B = 12229.686$$

Step 4) Propagating the distributed moments toward A and E. For example,

Table 1 Step-by-step process of rotation propagation, example 1

Nodes	A	B			C			D		E
ij	AB	BA	BF	BC	CB	CG	CD	DC	DH	DE	ED
C^θ	-0.10750	-0.30513	0	**0.13099**	-0.11668	-0.11961	**-0.12312**	-0.13088	0	-0.36917	-0.11961
M_i	0	**33576.424**			**-60923.576**				0		0
K_i	0.034798	**0.098777**			**0.087985**				0.093534		0.030304
θ_B^B	-	**339920.02**			-				-		-
$\theta_B^{i\neq B}$	-103720.9	-			**-44526.35**				**5481.906**		-2023.736
θ_C^C	-	-			**-692431.9**				-		-
$\theta_C^{i\neq C}$	-24652.32	80791.949			-				**85249.442**		-31471.24
$\sum\theta_i$	-128373.3	420711.96			-736958.3				**90731.348**		-33494.98

Table 2 Step-by-step process of moment propagation, example 2

Nodes	A		B			C			D		E
ij	AB	BA	BF	BC	CB	CG	CD	DC	DH	DE	ED
C_M	0.20434	0		0.25028	**0.26385**		0.25777	0.25038		0	0.26109
$C_{M'}$	-0.11114	0		-0.11889	**-0.13837**		-0.14637	-0.11878		0	-0.14200
$C_{M''}$	-0.093201	0		-0.13139	**-0.12549**		-0.11140	-0.13160		0	-0.11907
D^i or D'^i	1	0.33032	0.36423	**0.30544**	**0.34481**	0.311233	0.343958	0.32258	0.38465	0.29276	1
M_F	0	0	0	**-33576.424**	**60923.576**	0	0	0	0	0	0
DM_B	-	11091.024	12229.686	**10255.714**	-	-	-	-	-	-	-
PM_B	0	-	-	-	2566.787	-1219.280	-1347.507	-347.342	197.229	150.113	0
DM_C	-	-	-	-	**-21007.327**	-18961.093	-20955.156	-	-	-	-
PM_C	0	2636.107	2906.743	**-5542.850**	-	-	-	-5401.529	3067.115	2334.414	0
$M^{mn}=\sum M$	0	13727.13	15136.43	**-28863.56**	42483.04	-20180.37	-22302.66	-5748.87	3264.34	2484.53	0

Table 3 Step-by-step process of moment propagation, example 3

Nodes	A	B		C		D		E			F	G
ij	AB	BA	BC	CB	CD	DC	DE	ED	EF	FE	FG	GF
C_M	0.14479	0	0.19136	0.20072	0.19184	**0.19169**	0.20501	0.19135	0.15038	0.15443	0.36917	0
D^i	1	0.52547	0.47453	0.50088	**0.49912**	**0.498673**	0.50133	0.46165	0.53581	0.51924	0.48076	0
M^F	0	0	0	0	**-2060.449**	**1539.551**	0	0	0	0	0	0
DM_C	-	-	-	1032.043	**1028.405**	-	-	-	-	-	-	-
PM_C	0	-207.147	207.147	-	-	197.292	-197.292	-40.446	40.446	6.082	-6.082	-2.245
DM_D	-	-	-	-	-	**-767.733**	-771.818	-	-	-	-	-
PM_D	0	-29.538	29.538	147.163	**-147.163**	-	-	-158.229	158.229	23.794	-23.794	-8.784
$M^{mn}=\sum M$	0	-236.68	236.68	1179.21	**-1179.21**	969.11	-969.11	-198.67	198.67	29.88	-29.88	-11.03

$$PM_B^{AB} = DM_B^{BA}.C_M^{BA} = 0.,$$
$$PM_B^{CB} = DM_B^{BC}.C_M^{BC} = 2566.787$$
$$PM_B^{CG} = DM_B^{BC}.C_{M'}^{BC} = -1219.280,$$
$$PM_B^{CD} = DM_B^{BC}.C_{M''}^{BC} = -1347.507,$$

Step 5) Reiterating the steps 3 to 4 for the joint C. The results are available in Table 2,

Step 6) Adding the consequences of stages 3-5 and the fixed-end moments to achieve the final member-end moments, being accessible in the last row of Table 2.

Lay emphasis on that the moment propagation method is capable to calculate a single member-end moment by the moment closed-form equation of (32), directly. For example,

$$M^{BC} = M_{BC}^F + M_B^{BC} + \beta_L^{BC}[M_C^{CB}(1)] = -28863.56,$$

where $\beta_L^{BC} = C_M^{CB}$

The required moment propagation parameters and resulted moments to gain M^{BC} are available in Table 2 with bolded font. Note that for determination of M^{BC} by Dowell's equations, after calculating M^{BA} and M^{BF}, the moment equilibrium equation at joint B should be applied.

4.3 Example 3

Fig. 10 shows a continuous beam in which geometrical and mechanical properties of members are as the same as example 1. Herein, the member-end moments are directly determined using moment propagation process. The computed free-distribution and moment propagation factors are attainable in Table 3. Note that there is no column at all

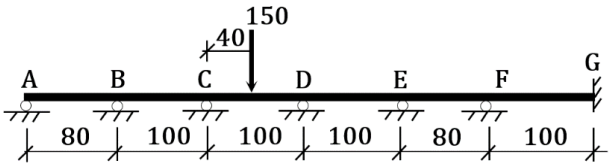

Fig. 10. A continuous beam for examples of 3-4.

joints, so the rotational stiffness of spring for each beam-spring model is equal to the rotational stiffness of its neighbor end of the previous beam-spring model ($K_i^R = K^{i(i+1)}$ & $K_i^L = K^{i(i-1)}$), and γ' will be zero, thus $C_M = -C_{M''}$. For example

$$C_M^{EF} = \frac{\gamma_F^R \alpha^{EF}}{\gamma_F^R + 1 - (\alpha^{EF})^2} = 0.369167 = -C_{M''}^{EF}$$

Also, due to the fixed-support taking place at G, K_F^R and γ_E^R will be infinite, so

$$C_M^{FG} = \frac{\gamma_G^R \alpha^{FG}}{\gamma_G^R + 1 - (\alpha^{FG})^2} = \alpha^{FG}$$

Pay attention, for computation of M^{CD}, only the bolded values in Table 3 are necessary. In addition, one can derive this moment from the moment closed-form equation as

$$M^{CD} = M_{CD}^F + M_C^{CD} + \beta_L^{CD}[M_D^{DC}(1)] = -1179.21,$$

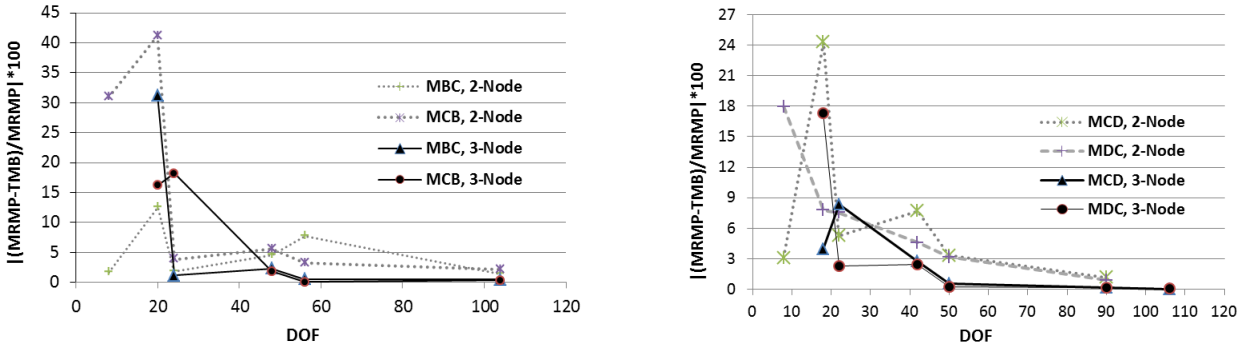

(a) The bridge frame error curves (b) The continuous beam error curves

Fig. 11. TMB-FE responses comparing to RMP

in which $\beta_L^{CD} = C_M^{DC}$

4.4 Example 4

A bridge-type structure is usually characterized by relatively concentrated convoy loads, and several load cases (Jansseune and Corte 2017). In this part, to investigate the effects of load change on volume of computations, the continuous beam of example 3 is subjected to a gravity point load of 180, located on span *BC*, at 1/3 from *B*. The solution involves only 1) computing the equivalent moments M_B=*2436.94* and M_C=*-3133.80*, and 2) putting them in the moment closed-form equation or the step-by-step procedure. Note that the required moment propagation parameters were previously calculated in example 3. For instance,

$$M^{CD} = (M_C)D^{CD} + (C_M^{BC})[(M_B)D^{BC}] = -1785.41979$$

4.5 Comparing RMP and TMB-FE results

In this stage, the bridge-type structures of the examples section are re-analyzed using a computer code written by the authors based on TMB-FE model. The structures were divided into a different number of elements, contributed to various degrees of freedoms (DOFs). Fig. 11 portrays the error curves of a sequence of models that involve changing in DOFs of the structure.

The error values convey the differences between the end-moments obtained by TMB-FE model and what derived by RMP method, in percent. One can observe that the moment estimation oscillatory converges to the response of the presented approach by rectifying the mesh, for instance, to reach to RMP accuracy by the 3-NE, the bridge frame should divide into at least 14 elements including 56 DOFs. Also, the convergence rate of the 2-NE is much less than 3-NE. Furthermore, using 3-NE, the errors are coming down from 31 and 17 percent to negligible amount for the bridge frame and the continuous beam, respectively, due to refining the mesh. Similarly, they are decreasing from 41 and 24 percent to insignificant values by applying 2-NE.

5. Conclusions

In this study, we derive a new formulation for calculation of exact member-end rotations or moments of bridge-type structures, individually, including both flexural and shear effects. A comparison is conducted to provide the superiority of RMP algorithm in respect to the algorithms of the methods available in the literature. The contributions show that contrary to RMP method; Dowell and Johnson's methodology needs help from the static moment equilibrium equations, moment distribution method involves successive moment balance, even for a single member-end rotation or moment and for each load case, and slope distribution method, which does not include shear effects, comprises an iterative algorithm resulting in inaccurate responses. Moreover, certifying numerical examples show that RMP is simple, exact and in contrast to TMB-FE scheme does not require a mesh of discrete elements leading to a set of equations, which should be solved, simultaneously. Moreover, the results computed by the TMB-FE method converge in the RMP responses, in a fluctuating manner, when the mesh includes 14 elements of 3-node, comprising 56 DOFs.

These superiorities make highlight the capability of RMP in general practical cases, where a bridge-type structure bears several load patterns and (or) has many indeterminacies.

Acknowledgments

The authors gratefully acknowledge the University of Zabol, which partially supported this research.

References

Almayah, A.A. (2018), "Simplified analysis of continuous beams", *J. Appl. Eng. Res.*, **13**(2), 922-928.

Cross, H. (1932), "Analysis of continuous frames by distributing fixed-end moments", *American Soc Civil Eng. Trasactions*, **96**(1793), 1-10.

Dowell, R.K. (2009), "Closed-form moment solution for continuous beams and bridge structures", *Eng. Struct.*, **31**(8), 1880-1887. https://doi.org/10.1016/j.engstruct.2011.09.023.

Dowell, R.K. and Johnson, T.P. (2011), "Shear and bending flexibility in closed-form moment solutions for continuous beams and bridge structures", *Eng. Struct.*, **33**(12), 3238-3245. https://doi.org/10.1016/j.engstruct.2011.08.016.

Dowell, R.K. and Johnson, T.P. (2012), "Closed-form shear flow solution for box–girder bridges under torsion", *Eng. Struct.*, **34**, 383-390.

Eslami, M.R. (2014), *Finite Elements Methods in Mechanics*, Springer International Publishing, Switzerland.

Gere, J.M. (1963), *Moment Distribution*, Van Nostrand, U.S.A.

Hosseini-Tabatabaei, M. and Rezaiee-Pajand, M. (2012), "Analysis of continuous beams and bridge frames based on propagating rotations", *J. Iran. Soc. Civ. Eng.*, **14**(34), 53-61.

Hosseini-Tabatabaei, M., Rezaiee-Pajand, M. and Mollaei-Nia, M. (2017), "Analysis of continuous beams and bridge frames using moment propagation", *J. Iran. Soc. Civ. Eng.*, **19**(46), 74-83.

Jansseune, A. and Corte, W.D. (2017), "The influence of convoy loading on the optimized topology of railway bridges", *Struct. Eng. Mech.*, **64**(1), 45-58. https://doi.org/10.12989/sem.2017.64.1.045.

Karttunen, A.T., Romanoff, J. and Reddy, J.N. (2016), "Exact microstructure-dependent Timoshenko beam element", *Int. J. Mech. Sci.*, **111**(112), 35-42. https://doi.org/10.1016/j.ijmecsci.2016.03.023.

Kaya, Y. and Dowling, J. (2016), "Application of Timoshenko beam theory to the estimation of structural response", *Eng. Struct.*, **123**, 71-76. https://doi.org/10.1016/j.engstruct.2016.05.026.

Mirfallah, S.M.H. and Bozorgnasab, M. (2015), "A new Jacobi-based iterative method for the classical analysis of structures", *Latin American J. Solids Struct.*, **12**, 2581-2617. http://dx.doi.org/10.1590/1679-78251993.

Regueiro, R.A. and Duan, Z. (2015), "Static and dynamic micropolar linear elastic beam finite element formulation, implementation, and analysis", *J. Eng. Mech.*, **141**(8), 1-18. https://ascelibrary.org.doi/10.1061/(ASCE)EM.1943-889.0000910.

Romanoff, J., Reddy, J.N. and Jelovica, J. (2016), "Using non-local Timoshenko beam theories for prediction of micro- and macro-structural responses", *Compos. Struct.*, **156**, 410-420. https://doi.org/10.1016/j.compstruct.2015.07.010.

Tabsh, S.W. and Mitchell, M.M. (2016), "Girder distribution factors for steel bridges subjected to permit truck or super load", *Struct. Eng. Mech.*, **60**(2), 237-249. https://doi.org/10.12989/sem.2016.60.2.237.

Zuraski, P.D. (1991), "Continuous-beam analysis for highway bridges", *J. Struct. Eng.*, **117**(1), 80-99. https://doi.org/10.1061/(ASCE)0733-9445(1991)117:1(80).

CC

Appendix

$$[S]_{2-\text{node}} = \begin{bmatrix} 3S_2 & & S & \\ 3S_1 & 3S_4+10S_3 & Y & \\ -6S_2 & -3S_1 & 6S_2 & M \\ 3S_1 & -3S_4+5S_3 & -3S_1 & 3S_4+10S_3 \end{bmatrix} \tag{A-1}$$

$$[S]_{3-\text{node}} = \begin{bmatrix} 7S_2 & & & & & \\ 3S_1 & S_5 & & S & & \\ -8S_2 & -4S_1 & 16S_2 & & Y & \\ 4S_1 & S_6 & 0 & S_8 & & M \\ S_2 & S_1 & -8S_2 & -4S_1 & 7S_2 & \\ -S_1 & S_7 & 4S_1 & S_6 & -3S_1 & S_5 \end{bmatrix} \tag{A-2}$$

$$\begin{aligned} &S_1 = \frac{GA}{6c_S},\ S_2 = \frac{GA}{6Lc_S},\ S_3 = \frac{GAL}{30c_S}, \\ &S_4 = \frac{EI}{3L},\ S_5 = 7S_4 + 3S_3,\ S_6 = -8S_4 + 2S_3, \\ &S_7 = S_4 - S_3,\ S_8 = 16(S_4 + S_3) \end{aligned} \tag{A-3}$$